Optica Applicata, Vol. LI, No. 4, 2021
DOI: 10.37190/oa210412

Effect of linewidth enhancement factor (LEF) on routes to chaos in optically injected semiconductor lasers

N.M. Al-Hosiny

Department of Physics, College of Science, Taif University,
P.O. Box 11099, Taif 21944, Saudi Arabia;
nalhosiny@yahoo.co.uk

The effect of the linewidth enhancement factor (LEF) or α-factor on two common routes to chaos (mainly period-doubling and quasi-periodic routes) in optically injected semiconductor laser is theoretically investigated using bifurcation diagrams. The value of the LEF is slightly modified to examine the sensitivity of routes to chaos to any variation in the LEF. Despite the fact that LEF enhances chaos in the system, both routes are found to be highly insensitive to the variation in the LEF.

Keywords: injection locking, chaos, linewidth enhancement factor, routes to chaos.

1. Introduction

The linewidth enhancement factor (LEF) or the Henry factor [1] is considered as one of the main characters that distinguishes the behavior of semiconductor lasers with respect to other types of lasers. This factor is also known as α-factor, chirp factor, or the phase -amplitude factor [2]. LEF has been in intensive investigation since 1982 [3–5]. Using the self- mixing method, Guiliani *et al*. [6] showed that for some lasers the α-factor varies with the emitted power, and this variation can be correlated with the variations in the laser linewidth. This factor has also shown a large influence on fiber dispersion used in optical fiber communication system [7]. Various methods have been proposed to measure this factor including self-mixing [6, 8] and different optical feedback techniques [9]. Interestingly, a zero LEF has been observed in quantum dot lasers [10] which opens the door for the enhancement of device characteristics. It is also shown in quantum dot lasers, that optical injection strongly changes the behavior of the LEF [11]. The manipulation of the LEF has also been reported in an injection-locked quantum -dash Fabry–Pérot laser [12].

In terms of the nonlinear dynamics of semiconductor lasers including stability, instability and chaos, the LEF seems to play a major role in this aspect. In a previous

work [13], we showed theoretically that the LEF has huge impact on the stability map. In particular, the chaotic behavior is shown to be boosted as the LEF increases, which can be utilized in cryptogaphical communications. The LEF has also been found to play a key role in time-delay signature (TDS) in chaotic semiconductor ring lasers (SRL), which can also be useful in optical chaotic secure communications [14]. Another recent study [15] has shown that varying the LEF leads to the creation of discontinuities through disaggregation from the so-called shrimp-like structures.

Chaotic synchronization has been increasingly devoted to very recent investigation due to its possible utilization in communication security and broadband data transition [16, 17]. The dynamical system in semiconductor lasers or any other systems transfer from stability to chaos through a successive behavior called routes to chaos [18]. A very recent study has introduced a general review of experimental investigation of the routes to chaos in semiconductor laser subjected to optical feedback from a distant reflector, including period-doubling, quasi-periodic and subharmonic routes [19]. These routes as well as the chaos itself and other dynamical behaviors, can be studied using bifurcation diagram where we observe how the system changes and reacts [20, 21]. This bifurcation has been used theoretically and experimentally to study the dynamics of semiconductor lasers [22–25].

In this article, we theoretically investigate the effect of the LEF on routes to chaos, mainly period-doubling (PD) and quasi-periodic (QP) routes using bifurcation diagrams.

2. Model

Our model used in this study is a standard optical injection model [26], where the output of a single-mode semiconductor laser (known as the master laser, ML) is injected into the cavity of another single-mode semiconductor laser (known as the slave laser, SL). There are two major parameters that control the dynamics of the whole system. These parameters are the injection strength K and frequency detuning Δf. The injection strength is an indication of how much power is injected and can be defined as the electric field of ML relative to the electric field of the SL, (*i.e.*, $K = E_1/E_o$, where E_1 is the electric field of the ML and E_o is the electric field of the SL). The frequency detuning is defined as the difference between the frequency of ML and SL, (*i.e.*, $\Delta f = f_1 - f_o$, where f_1 is the frequency of ML and f_o is the frequency of the SL).

In this study, we use the model presented in [26], which is based on Lang's approach. The rate equations are numerically integrated using the Runge–Kutta method to calculate population inversion, electric field and phase. The theoretical power spectra are then generated by applying fast Fourier transform (FFT) to a chosen time window of the SL electric field time series using a computer software (Matlab). Recording the extrema of the electric field while running the model generates the bifurcation diagrams. The bifurcation diagrams were plotted for the extrema of the electric field as a function of K for different operational points to examine the LEF on the routes to chaos. All the

T a b l e. Parameters used in our simulation as experimentally characterized [26].

Parameter	Value
Wavelength λ	1556.6 nm
Differential gain G_N	1.4×10^{-12} m^3 s^{-1}
Carrier lifetime τ_s	0.43 ns
Photon lifetime τ_p	1.8 ps
Coupling rate η	9×10^{10} s^{-1}
Transparency carrier density N_o	1.1×10^{24} m^{-3}
Threshold carrier density N_{th}	1.5×10^{24} m^{-3}
Normalized injection current I/I_{th}	2

parameters used in our simulation were experimentally characterized in a previous study as shown in the Table and described in detail in [26].

3. Results and discussion

To examine the effect of the LEF on the routes to chaos, we first draw the theoretical dynamics map of the optically injected semiconductor laser at a standard value of α (that is when $\alpha = 3$). The dynamics map or stability map [26] is a two dimensional map showing the behavior of the laser when changing the injection level K and the frequency detuning Δf. This map, which is shown in Fig. 1, is published in our previous work [27]. The white region indicates the stable region S, where the laser does not exhibit any dynamics rather than a single and stable locked peak (where the slave laser is completely

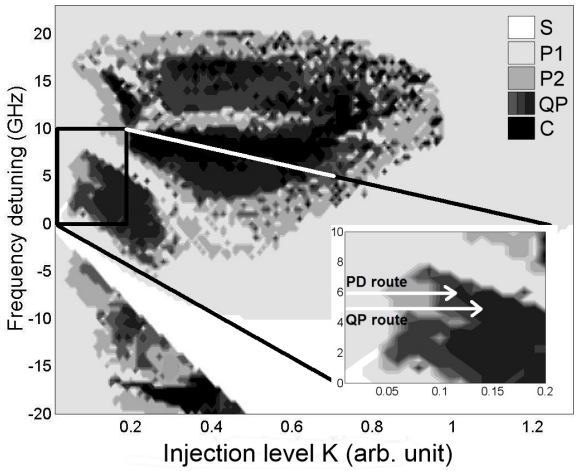

Fig. 1. Stability map of the SL. The colors indications are as shown in the figure where, S is stable locking, P1 is the period one dynamics, P2 is the period two dynamics, QP is the quasi-periodic dynamics and C is chaos. The inset is a magnified part of the small chaotic island where the PD and QP routes are indicated by white arrows.

locked to the master [28, 29]). The very white grey indicates the period-one (P1) behavior or the so-called limit-cycle or self-oscillation [30], where a closed trajectory is clearly spotted in the phase space of the system (the fundamental frequency as the period). If a new limit-cycle is emerged from an existing limit-cycle, with the period that is double of the old one, the period-doubling (P2 or PD) behavior is then obtained [31], which is indicated in the figure by the grey color. However, when the system shows irregular periodicity, we call this behavior the quasi-periodic (QP) behavior, which is indicated in the figure by the dark grey color. Finally, the chaotic behavior is shown in the black region. Further discussion of this map with its experimental verification can be found in our previous work [27].

The inset of Fig. 1 shows the small chaotic island where we examine our two chosen routes to chaos (the PD and QP routes). The system evolves from stability to chaos and shows rich nonlinear dynamics and we shall investigate these two routes and see the effect of the LEF on them.

3.1. Period-doubling route

Figure 2 shows the bifurcation diagram of the PD route when $\alpha = 3$. This diagram is plotted by recording the extreme of the SL electric field as a function of the injection level K at the chosen frequency detuning ($\Delta f = 6$ GHz). As shown in the figure, the system bifurcates in a doubling manner till reaching chaos. The labels *a*–*e* shown in this figure correspond to the dynamics illustrated in Fig. 3, where we plot the dynamics of the route in three columns; the power spectra (in logarithmic scale), the electric field time series and the population inversion *versus* electric field, respectively.

In order to examine the effect of LEF on the PD routes, we tried to vary the value of the LEF for different possible values (that is, 2.4, 2.6, 2.8, 3.2, 3.4 and 3.6). In each

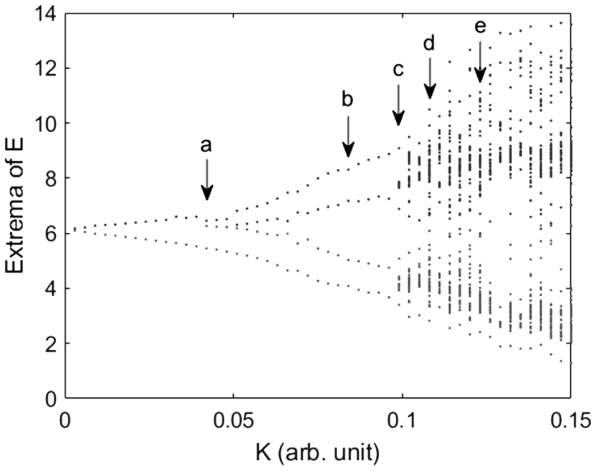

Fig. 2. Bifurcation diagram of the SL dynamics as a function of the injection strength K for the PD route at $\Delta f = 6$ GHz as shown in the inset of Fig. 1. The labels represent the operating points at which the dynamics shown in Fig. 3 are plotted.

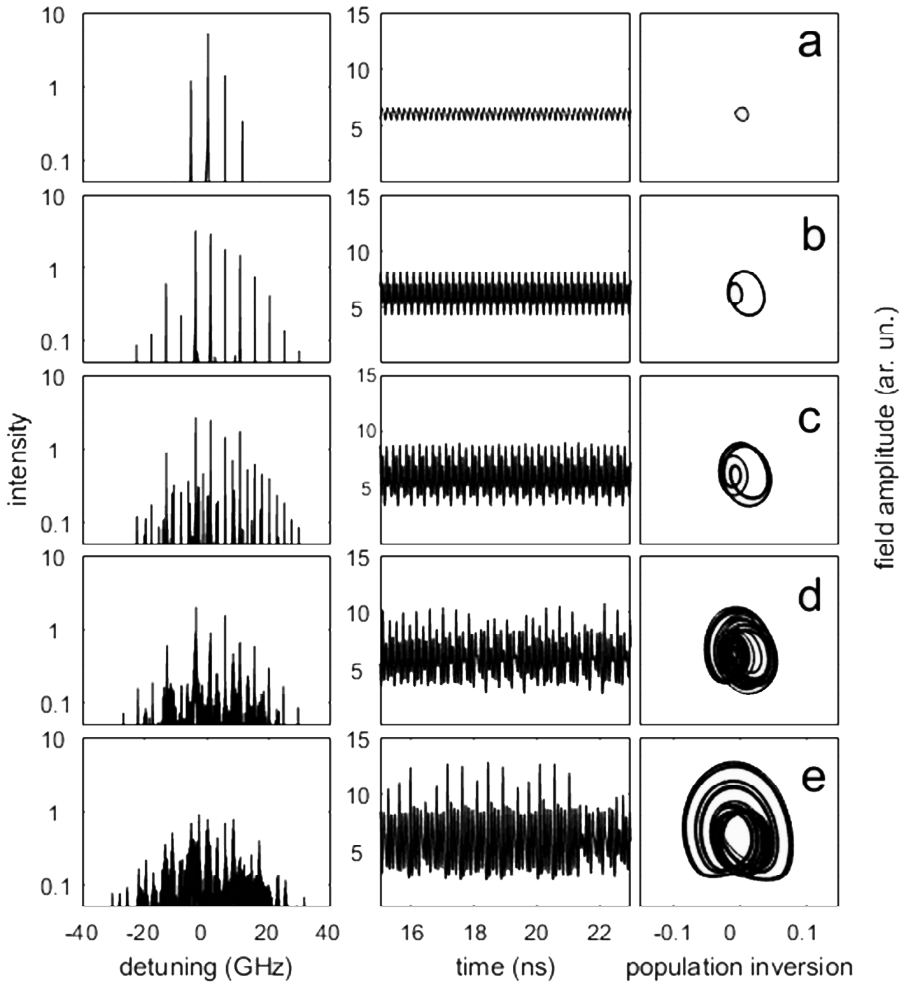

Fig. 3. The power spectra (first column), the electric field time series (second column) and the population inversion *versus* electric field (third column) for the operating points shown in Fig. 2.

case, we run the system and draw the bifurcation diagrams (as we fix Δf at 6 GHz and raise the injection power K) along with the route dynamics shown in Fig. 2. The standard value that is used in our model for the LEF is 3 as mentioned before, so we systematically chose three values below 3 and other three values above 3. The step between these values is meant to be small so that the whole dynamics map does not change significantly. Choosing high or low values of LEF could lead to a considerable change so that the chaotic island (where we examine the routes) may totally disappear, see [13] for more details. Therefore, the change in LEF was meant to be small to investigate the sensitivity of the routes to any variation in the LEF.

Figure 4 shows the bifurcation diagrams for the six values of the LEF. It can be seen from the figure that the route gets shorter (the chaos appears at lower injection level)

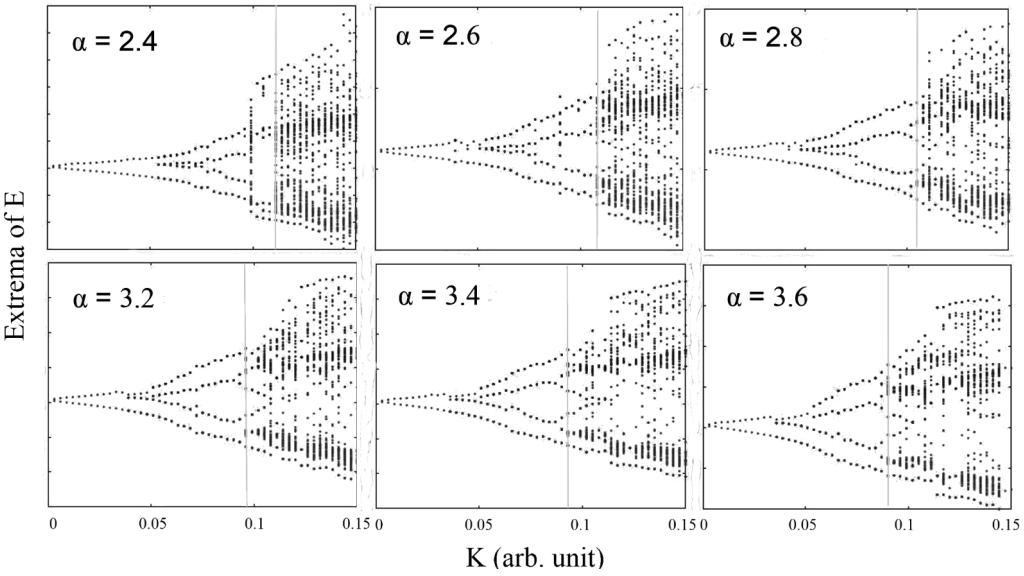

Fig. 4. Bifurcation diagrams of the PD route when the LEF is changed from 2.4 to 3.6. Note that Δf = = 6 GHz and K is the varied parameter in the bifurcation diagrams.

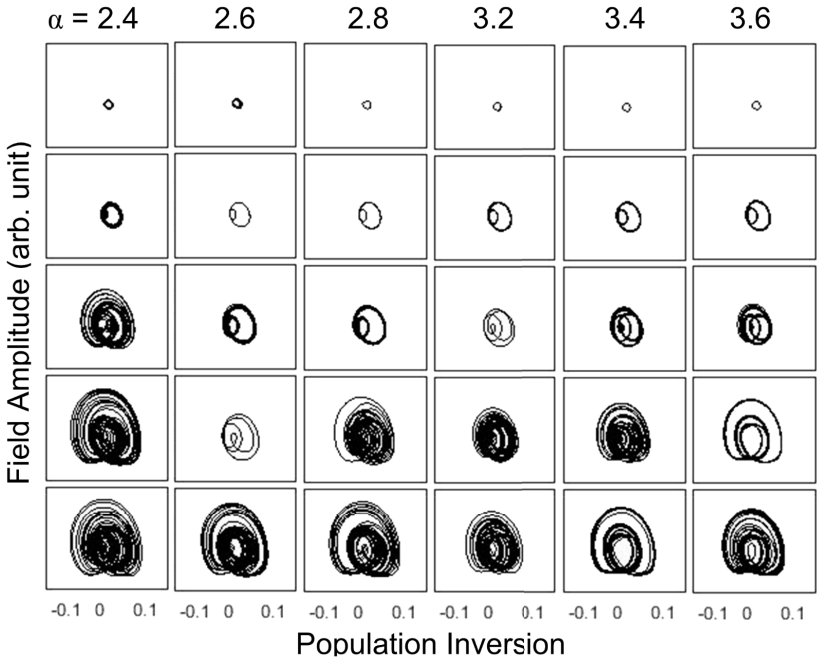

Fig. 5. The population inversion *versus* electric field for the PD route at different values of the LEF (columns), when K = 0.04, 0.08, 0.99, 0.112, 0.12 (rows), respectively.

as the value of the LEF increases. Note that chaos can be recognized by the appearance of many peaks in the spectra, *i.e.* many dots in the bifurcation diagrams at a point in which there is no sign for the route anywhere behind. These points are roughly indicated by the grey lines in the figure. This shortness of the routes and the appearance of chaos earlier is clearly due to the fact that the LEF enhances the nonlinear dynamics in general [13], which means that the chaos island shown in the inset of Fig. 1 becomes slightly bigger as the value of the LEF increased. In terms of the PD route itself, it seems that the route is not noticeably affected by the changing of the LEF. That is to say, although the LEF enhances the chaotic behavior, the transition routes to chaos remain almost unaffected and the doubling behavior is still evident in all cases.

To have a closer look at the PD route under these values of the LEF, we plotted the population inversion as a function of field amplitude when $K = 0.04$, 0.08, 0.99, 0.112, and 0.12 (these are the rows), as shown in Fig. 5. The series of K values are chosen according to bifurcation diagrams for the best illustration of the route and kept the same so we can see the sensitivity of the route to the change in the LEF. Again, the route in general seems not to be affected by changing the LEF. However, the route looks ideal in some cases (at $\alpha = 2.6$ and 3.6). This might be attributed to the chosen operating point rather than to any other reasons.

3.2. Quasi-periodic route

The QP route is another famous route to chaos where the system evolves to chaos in a quasi-periodic manner as we described before. Figure 6 shows the bifurcation diagram of the QP route when $\alpha = 3$. This bifurcation diagram is plotted at frequency detuning $\Delta f = 5$ GHz, which corresponds to the route as shown in the inset of Fig. 1.

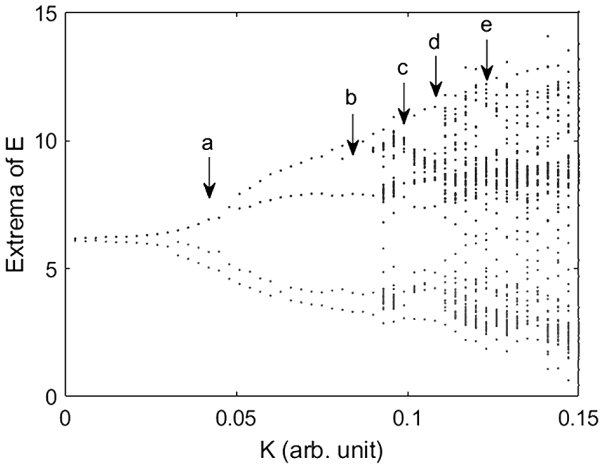

Fig. 6. Bifurcation diagram of the SL dynamics as a function of the injection strength K for the QP route at $\Delta f = 5$ GHz as shown in the inset of Fig. 1. The labels represent the operating points at which the dynamics shown in Fig. 7 are plotted.

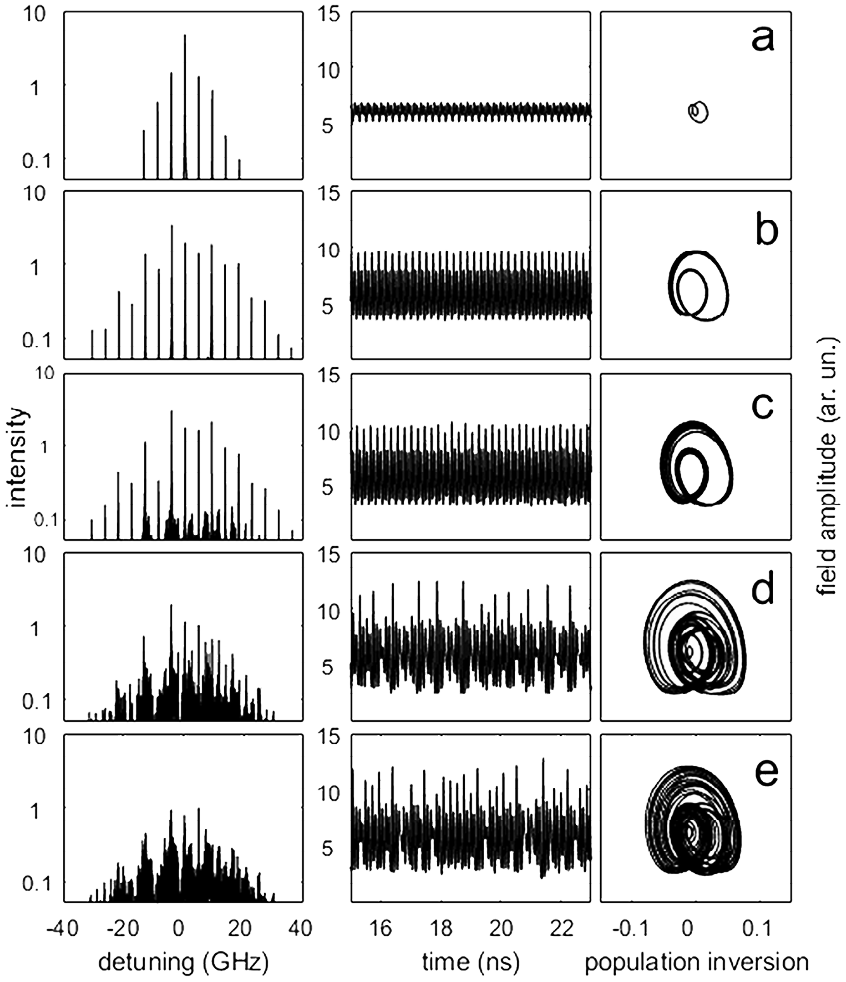

Fig. 7. The power spectra (first column), the electric field time series (second column) and the population inversion *versus* electric field (third column) for the operating points shown in Fig. 6.

Likewise, the labels *a–e* shown in this figure correspond to the dynamics illustrated in Fig. 7. The periodic behavior is clearly shown in the bifurcation diagram and also in the power spectra, the time series and the population inversion. This behavior can be distinguished by the appearance of additional peaks in a systematic manner, *i.e.* that is the appearance of two incommensurate frequencies. This can also be noticed in the electric field time series as different periods and in the population inversion trajectory as additional circles. In contrast to the QP behaviors, the chaotic behavior can be recognized as the emergent of many peaks in a hectic manner. That is reflected on the electric field time series and population inversion trajectory as complete mess with no sign of order or periodicity.

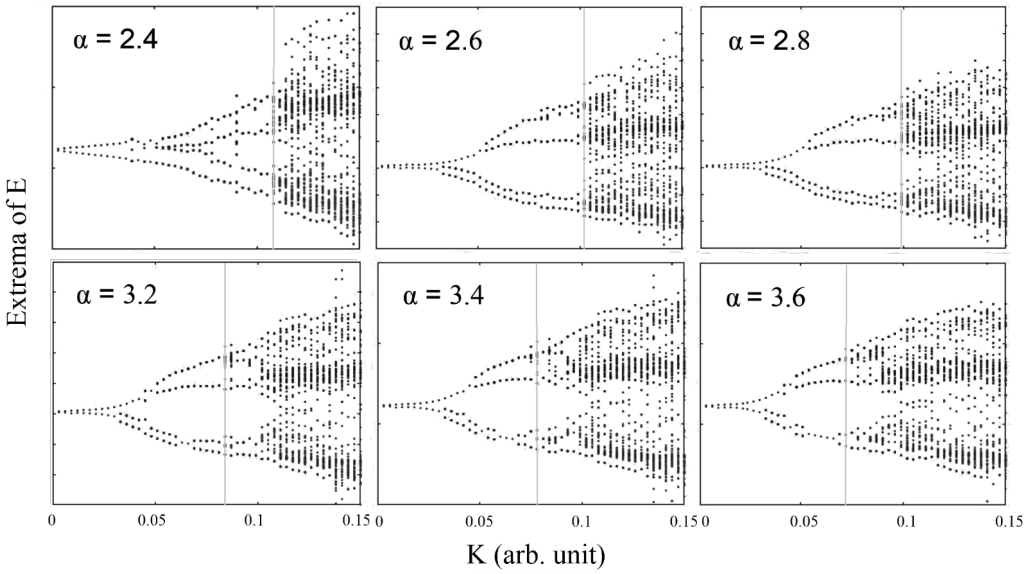

Fig. 8. Bifurcation diagrams of the QP route when the LEF is changed from 2.4 to 3.6. Note that Δf = = 5 GHz and K is the varied parameter in the bifurcation diagrams.

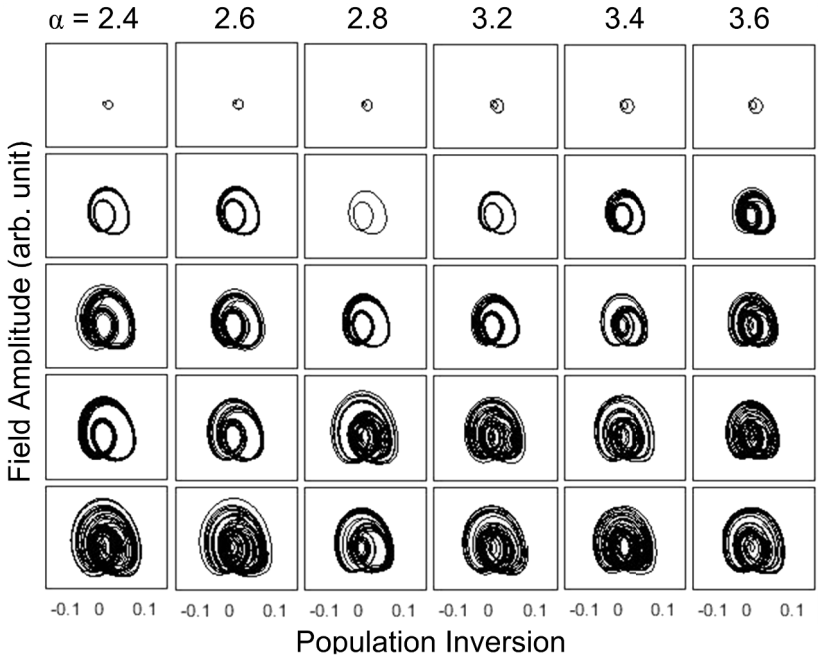

Fig. 9. The population inversion *versus* electric field for the QP route at different values of the LEF (columns), when K = 0.04, 0.08, 0.99, 0.112, 0.12 (rows), respectively.

We repeat the same examination by plotting the bifurcation diagrams at the six different values of the LEF. Figure 8 shows the bifurcation diagrams at the chosen values of the LEF for the QP route. Once more, as the LEF increases, the QP route becomes shorter and the chaos is reached earlier for the same reason mentioned before. As the previous route, the QP route seems to be more or less independent when changing the LEF. This fact is further proved by plotting the population inversion as a function of field amplitude (when $K = 0.04$, 0.08, 0.99, 0.112, and 0.12) as shown in Fig. 9.

We can see that routes to chaos almost maintain themselves regardless of the modification in the stability map (*i.e.* the slight change in the LEF). This raises more questions about the dynamics itself and the carrier density inside the laser cavity, which can be investigated in future along with the attempt to verify these findings experimentally.

4. Conclusions

We have theoretically investigated the effect of the LEF on two common routes to chaos (PD and QP). Using bifurcation diagrams, we showed that as the LEF enhances nonlinear dynamics in the system, both routes to chaos appear to be unaffected by the variation in the LEF factor. This independence could be utilized in some communication applications where the routes to chaos are used in optical synchronization. Further experimental verification of this relation between the LEF and the routes to chaos is recommended.

Acknowledgements – The author appreciates the help and support of Taif University Researchers, the support number: TURSP-2020/25, Taif University, Taif, Saudi Arabia. Aljouf University is also thanked for their support.

References

[1] Henry C., *Theory of the linewidth of semiconductor lasers*, IEEE Journal of Quantum Electronics **18**(2), 1982, pp. 259–264, DOI: 10.1109/JQE.1982.1071522.

[2] Chuang C.F., Liao Y.H., Lin C.H., Chen S.Y., Grillot F., Lin F.Y., *Linewidth enhancement factor in semiconductor lasers subject to various external optical feedback conditions*, Optics Express **22**(5), 2014, pp. 5651–5658, DOI: 10.1364/OE.22.005651.

[3] Harder C., Vahala K., Yariv A., *Measurement of the linewidth enhancement factor a of semiconductor lasers*, Applied Physics Letters **42**(4), 1983, pp. 328–330, DOI: 10.1063/1.93921.

[4] Henning I.D., Collins J.V., *Measurements of the semiconductor laser linewidth broadening factor*, Electronics Letters **19**(22), 1983, pp. 927–929, DOI: 10.1049/el:19830633.

[5] Yu Y., Giuliani G., Donati S., *Measurement of the linewidth enhancement factor of semiconductor lasers based on the optical feedback self-mixing effect*, IEEE Photonics Technology Letters **16**(4), 2004, pp. 990–992, DOI: 10.1109/LPT.2004.824631.

[6] Giuliani G., Donati S., Elsässer W., *Measurement of linewidth enhancement factor of different semiconductor lasers in operating conditions*, Proceedings of SPIE **6184**, 2006, article 61841D, DOI: 10.1117/12.665178.

[7] Liu Z.Y., Zhao T.G., *Effect of linewidth enhancement factor in semiconductor laser on fiber dispersion transmission system*, [In] *2015 Fifth International Conference on Instrumentation and Measurement, Computer, Communication and Control (IMCCC)*, Qinhuangdao, China, September 18–20, 2015, DOI: 10.1109/IMCCC.2015.153.

[8] Fan Y., Yu Y., Xi J., Rajan G., Guo Q., Tong J., *Simple method for measuring the linewidth enhancement factor of semiconductor lasers*, Applied Optics **54**(34), 2015, pp. 10295–10298, DOI: 10.1364/AO.54.010295.

[9] Jumpertz L., Michel F., Pawlus R., Elsässer W., Schires K., Carras M., Grillot F., *Measurements of the linewidth enhancement factor of mid-infrared quantum cascade lasers by different optical feedback techniques*, AIP Advances **6**(1), 2016, article 015212, DOI: 10.1063/1.4940767.

[10] Zubov F.I., Maximov M.V., Moiseev E.I., Savelyev A.V., Shernyakov Y.M., Livshits D.A., Kryzhanovskaya N.V., Zhukov A.E., *Observation of zero linewidth enhancement factor at excited state band in quantum dot laser*, Electronics Letters **51**(21), 2015, pp. 1686–1688, DOI: 10.1049/el.2015.2512.

[11] Wang C., Chaibi M.E., Huang H.M., Erasme D., Poole P., Even J., Grillot F., *Frequency-dependent linewidth enhancement factor of optical injection-locked quantum dot/dash lasers*, Optics Express **23**(17), 2015, pp. 21761–21770, DOI: 10.1364/OE.23.021761.

[12] Naderi N.A., Pochet M.C., Grillot F., Shirkhorshidian A., Kovanis V., Lester L.F., *Manipulation of the linewidth enhancement factor in an injection-locked quantum-dash Fabry-Perot laser at 1550nm*, [In] *2010 23rd Annual Meeting of the IEEE Photonics Society*, Denver, CO, USA, November 7–11, 2010, DOI: 10.1109/PHOTONICS.2010.5698942.

[13] Al-Hosiny N.M., *Effect of linewidth enhancement factor on the stability map of optically injected distributed feedback laser*, Optical Review **21**(3), 2014, pp. 261–264, DOI: 10.1007/s10043-014-0038-5.

[14] Li J.F., Xiang S.Y., Wen A.J., Zhang H.X., Zhang H., Guo X.X., *Role of linewidth enhancement factor on time-delay signature concealment of chaos in mutually-coupled semiconductor ring lasers*, [In] *2016 25th Wireless and Optical Communication Conference (WOCC)*, Chengdu, China, May 21–23, 2016, DOI: 10.1109/WOCC.2016.7506620.

[15] Chávez C.A.T., Curilef S., *Discontinuous spirals of stability in an optically injected semiconductor laser*, Chaos **30**(5), 2020, article 053107, DOI: 10.1063/1.5119808.

[16] Al Bayati B.M., Ahmad A.K., Al Naimee A.M., *Effect of control parameters on chaos synchronization by means of optical feedback*, Optics Communications **472**, 2020, article 126032, DOI: 10.1016/j.optcom.2020.126032.

[17] Senlin Y., *Chaotic synchronization of mutually coupled lasers with another laser and its encoding application in secret communication*, Journal of Optical Communications, 2020, DOI: 10.1515/joc-2019-0225.

[18] Al-Hosiny N.M., *Sensitivity of routes to chaos in optically injected semiconductor lasers*, Journal of Nonlinear Optical Physics & Materials **23**(03), 2014, article 1450036, DOI: 10.1142/S0218863514500362.

[19] Locquet A., *Routes to chaos of a semiconductor laser subjected to external optical feedback: a review*, Photonics **7**(1), 2020, article 22, DOI: 10.3390/photonics7010022.

[20] Wieczorek S., Krauskopf B., Lenstra D., *A unifying view of bifurcations in a semiconductor laser subject to optical injection*, Optics Communications **172**(1–6), 1999, pp. 279–295, DOI: 10.1016/S0030-4018(99)00603-3.

[21] Wieczorek S., Chow W.W., *Bifurcations and chaos in a semiconductor laser with coherent or noisy optical injection*, Optics Communications **282**(12), 2009, pp. 2367–2379, DOI: 10.1016/j.optcom.2009.02.060.

[22] Wang H., Jiang W., Ding Y., *Bifurcation phenomena and control analysis in class-B laser system with delayed feedback*, Nonlinear Dynamics **79**, 2015, pp. 2421–2438, DOI: 10.1007/s11071-014-1822-2.

[23] Jahanpanah J., Rezazadeh M., Rahdar A.A., *Formation mechanism of bifurcation in mode-locked class-B laser*, Chinese Physics B **23**(12), 2014, article 124205, DOI: 10.1088/1674-1056/23/12/124205.

[24] Kim B., Locquet A., Li N., Choi D., Citrin D.S., *Bifurcation-cascade diagrams of an external-cavity semiconductor laser: experiment and theory*, IEEE Journal of Quantum Electronics **50**(12), 2014, pp. 965–972, DOI: 10.1109/JQE.2014.2363568.

[25] MERCIER E., WOLFERSBERGER D., SCIAMANNA M., *Bifurcation to chaotic low-frequency fluctuations in a laser diode with phase-conjugate feedback*, Optics Letters **39**(13), 2014, pp. 4021–4024, DOI: 10.1364/OL.39.004021.

[26] AL-HOSINY N.M., HENNING I.D., ADAMS M.J., *Correlation of electron density changes with optical frequency shifts in optically injected semiconductor lasers*, IEEE Journal of Quantum Electronics **42**(6), 2006, pp. 570–580, DOI: 10.1109/JQE.2006.874754.

[27] AL-HOSINY N.M., HENNING I.D., ADAMS M.J., *Tailoring enhanced chaos in optically injected semiconductor lasers*, Optics Communications **269**(1), 2007, pp. 166–173, DOI: 10.1016/j.optcom.2006.07.066.

[28] LANG R., *Injection locking properties of a semiconductor laser*, IEEE Journal of Quantum Electronics **18**(6), 1982, pp. 976–983, DOI: 10.1109/JQE.1982.1071632.

[29] HUI R., D'OTTAVI A., MECOZZI A., SPANO P., *Injection locking in distributed feedback semiconductor lasers*, IEEE Journal of Quantum Electronics **27**(6), 1991, pp. 1688–1695, DOI: 10.1109/3.89994.

[30] SIMPSON T.B., LIU J.M., ALMULLA M., USECHAK N.G., KOVANIS V., *Limit-cycle dynamics with reduced sensitivity to perturbations*, Physical Review Letters **112**(2), 2014, article 023901, DOI: 10.1103/PhysRevLett.112.023901.

[31] ERNEUX T., KOVANIS V., GAVRIELIDES A., ALSING P.M., *Mechanism for period-doubling bifurcation in a semiconductor laser subject to optical injection*, Physical Review A **53**(6), 1996, pp. 4372–4380, DOI: 10.1103/PhysRevA.53.4372.

Received December 23, 2020
in revised form March 22, 2021